Synthesis of Highly Reactive Polyisobutylene by FeCl3/Ether Complexes in Hexanes; Kinetic and Mechanistic Studies

ARTICLE · SEPTEMBER 2014

DOI: 10.1039/C4PY01039F

6 AUTHORS, INCLUDING:

Rajeev Kumar
University of Massachusetts Lowell
5 PUBLICATIONS **43** CITATIONS

SEE PROFILE

Bin Zheng
Xi'an University of Science and Technology
42 PUBLICATIONS **271** CITATIONS

SEE PROFILE

Polymer Chemistry

PAPER

View Article Online
View Journal

Cite this: DOI: 10.1039/c4py01039f

Synthesis of highly reactive polyisobutylene with $FeCl_3$/ether complexes in hexane; kinetic and mechanistic studies†

Rajeev Kumar,[a] Priyadarsi De,[b] Bin Zheng,[c] Kuo-Wei Huang,[c] Jack Emert[d] and Rudolf Faust*[a]

Received 28th July 2014,
Accepted 11th September 2014

DOI: 10.1039/c4py01039f

www.rsc.org/polymers

The kinetics and mechanism of the polymerization of isobutylene catalyzed by $FeCl_3$·ether complexes in hexane at 0 °C were investigated. The polymerization rates increased in the diisopropyl ether< 2-chloroethyl ethyl ether < bis(2-chloroethyl) ether order, attributed to electronic effects. The polymerization rates increased with increasing initiator and catalyst concentrations. The first order plots, however, deviated from the linear suggesting that the cation concentration decreases with time. The previously proposed mechanism is inadequate to explain this finding. The decrease in the polymerization rate with time is explained by the low solubility of the $H^+ROR'FeCl_4^-$ complexes that precipitate during polymerization. Based on mechanistic studies the revised mechanism now also includes the equilibrium $H^+ROR'FeCl_4^- \leftrightharpoons HCl + FeCl_3{\cdot}ROR'$.

Introduction

There is an increasing demand for polyisobutylene (PIB) based ashless dispersants for motor oil and fuel additives.[1] Lubricants or fuel dispersants are low molecular weight (M_n ~ 500–5000 g mol^{-1}), oil soluble PIB or polybutenes (copolymers of isobutylene (IB) with C4 olefins) with polar oligoamine end-groups.[2] The precursor polybutene or PIB olefins are generally produced by the $AlCl_3$ (or $EtAlCl_2$) catalyzed polymerization of a C4 mixture, or by BF_3 catalyzed IB polymerization.[3,4] Polybutenes contain an internal double bond, which has low reactivity towards maleic anhydride.[5] Therefore, a chlorination–dehydrochlorination procedure to create a diene moiety is required to react efficiently with maleic anhydride. However, the final product may contain up to 5000 ppm residual chlorine. PIB *exo*-olefin, which is obtained using a BF_3 complex with an ether or alcohol as a catalyst, readily reacts with maleic anhydride in a thermal "ene" reaction to produce PIB succinic anhydride and subsequently polyisobutenylsuccinimide ashless dispersants.[6] Because the final product does not contain any chlorine, this highly reactive (HR) PIB is more desirable than polybutenes.

Since BF_3 is detrimental for industrial equipment, and also requires low temperature to produce HR PIB, several methods have been developed in the recent past to obtain HR PIB.[7–9] Arguably the most promising catalyst system comprises a Lewis acid/Lewis base complex.[10] The latest development in new catalyst development for the synthesis of HR PIB has been reviewed recently.[11] The novel univalent gallium salts $[Ga(C_6H_5F)_2]^+[Al(OR^F)_4]^-$ and $[Ga(1,3,5\text{-}Me_3C_6H_3)_2]^+[Al(OR^F)_4]^-$ ($R^F = C(CF_3)_3$) were tested for initiating or catalyzing the synthesis of HR-PIB in several solvents.[12] Kostjuk *et al.* and Wu *et al.* reported the use of $AlCl_3$[13,14] and $FeCl_3$[15,16] ether complexes for the polymerization of IB in dichloromethane (DCM) or in DCM–hexane 80/20 (v/v) mixtures to give HR PIB with more than 90% *exo*-olefinic content in the molecular weight range of 1100–3500 g mol^{-1}. The use of a chlorinated solvent for the synthesis of HR PIB is the major drawback for this system, since rates and *exo*-olefin contents decrease with decreasing solvent polarity. In addition, only adventitious water has been shown to initiate the polymerization of IB in conjunction with the $AlCl_3$·ether complex.[17] We have reported the use of $GaCl_3$ or $FeCl_3$ ether complexes for the polymerization of IB in non-polar solvents in conjunction with conventional cationic initiators such as *tert*-butylchloride (*t*-BuCl),[18] and studied the steric and electronic effects of the ether structures on the polymerization rates and *exo*-olefin content.[19] The aim

[a]*Polymer Science Program, Department of Chemistry, University of Massachusetts Lowell, One University Avenue, Lowell, MA 01854, USA. E-mail: Rudolf_Faust@uml.edu*
[b]*Polymer Research Centre, Department of Chemical Sciences, Indian Institute of Science Education and Research Kolkata, Mohanpur – 741246, Nadia, West Bengal, India*
[c]*KAUST Catalysis Center and Division of Physical Sciences and Engineering, King Abdullah University of Science and Technology, Thuwal 2355-6900, Saudi Arabia*
[d]*Infineum USA, 1900 E. Linden Avenue, Linden, NJ 07036, USA*
† Electronic supplementary information (ESI) available: Table of polymerization data; calculated energies and Cartesian coordinates of all complexes. See DOI: 10.1039/c4py01039f

of this work is to probe the proposed polymerization mechanism *via* kinetic studies, and to find a system that provides fast polymerization and high *exo*-olefinic end group content.

Experimental section

Materials

Technical grade hexane (Doe & Ingalls) was refluxed over H_2SO_4 for 48 h, then washed with 10% KOH aqueous solution and finally washed with distilled water until the aqueous layer was neutral. The hexane was pre-dried by vigorously mixing with anhydrous Na_2SO_4 for 30 min and then refluxing over CaH_2 for 48 h. Then the hexane was distilled onto CaH_2, refluxed again for 24 h, and freshly distilled just before the polymerization reactions. Dichloromethane (DCM, 99.8%, Aldrich) was washed with 5% KOH aqueous solution and washed with distilled water until the aqueous layer was neutral. It was stored over Na_2SO_4 overnight and then refluxed for 12 h with CaH_2 and distilled onto phosphorus pentoxide (P_2O_5). It was refluxed again for 24 h and freshly distilled just before polymerization. Isobutylene (IB, Matheson Tri Gas) was dried by passing it through in-line gas-purifier columns packed with BaO/Drierite and then condensed in a receiver flask at −30 °C before use. 2-Methyl-d_3-propene-3,3,3-d_3 (IB-d_6, C/D/N Isotopes Inc., Canada, 98.3 atom % D), iron trichloride ($FeCl_3$, Aldrich 97%), *t*-BuCl (98%, TCI America) and P_2O_5 (98%, Alfa Aesar) were used as received. The IB-d_6 was condensed in a receiver flask at −50 °C before use. Diisopropyl ether (i-Pr_2O, anhydrous 99%), 2-chloroethyl ethyl ether (CEEE, 99%) and 2-chloroethyl ether (CEE, 99%) were purchased from Aldrich and used without any further purification. Cumyl chloride was prepared from cumyl alcohol (Aldrich, 97%) as reported elsewhere.[20]

Preparation of $FeCl_3$·dialkyl ether complexes in DCM

The $FeCl_3$·dialkyl ether complexes were prepared just before the polymerization of IB. In the glove box, DCM was added to $FeCl_3$, which had been previously weighed and sealed in a 20 mL vial with a Teflon septum. Next, an equimolar amount of the appropriate ether was added slowly *via* a syringe to the sealed vial containing the Lewis acid while stirring to form a 1.0 M Lewis acid/ether complex solution.

Polymerization of IB

Polymerization reactions were performed under a dry N_2 atmosphere in an MBraun glovebox (MBraun, Inc., Stratham, NH). IB was condensed and distributed to the polymerization reactors, screw top culture tubes (75 mL), at −30 °C. The polymerizations, which were co-initiated with $FeCl_3$/ether complexes at a monomer concentration of [IB] = 1.0 M, were performed in hexane at 0 °C and terminated with methanol (MeOH). Monomer conversion was determined gravimetrically.[21]

Characterization

Number average molecular weights ($M_{n,GPC}$) and polydispersity index (PDI) values were obtained from size exclusion chromatography (SEC) with universal calibration using a Waters 717 Plus auto-sampler, a 515 HPLC pump, a 2410 differential refractometer, a 2487 UV-VIS detector, a MiniDawn multi angle laser light scattering (MALLS) detector (measurement angles are 44.7°, 90.0°, and 135.4°) from Wyatt Technology Inc., a ViscoStar viscosity detector from Wyatt, and five styragelHR GPC columns connected in the following order: 500, 10^3, 10^4, 10^5 and 100 Å. The refractive index (RI) was the concentration detector. Tetrahydrofuran was used as the eluent at a flow rate of 1.0 mL min^{-1} at room temperature. The results were processed using the Astra 5.4 software from Wyatt Technology Inc. The attenuated total reflectance Fourier transform infrared spectroscopy (ATR FTIR) was performed using a Mettler–Toledo ReactIR 4000 instrument equipped with a DiComp probe connected to an MCT detector with a K6 conduit. The sampling wavenumbers were from 4000 to 650 cm^{-1} at a resolution of 2 cm^{-1}.

The proton nuclear magnetic resonance (^{1}H NMR) spectra were recorded on a Bruker 500 MHz spectrometer using $CDCl_3$ or CD_2Cl_2 as solvents (Cambridge Isotope Laboratories, Inc.). A typical ^{1}H NMR spectrum of HR PIB obtained in this study is shown in Fig. 1. The two protons characteristic of the *exo*-olefin end group (Structure I, protons a_1 and a_2) appear at 4.85 and 4.64 ppm, while the *endo*-olefin end group (Structure II, proton d) shows a peak at 5.15 ppm. Small amounts of the *E* and *Z* configurations of another tri-substituted olefin end group (Structure III, protons e_1 and e_2) could be noted at 5.37 and 5.17 ppm. The tetra-substituted olefin end group (Structure IV, proton f) appears as a broad multiplet at 2.85 ppm. Resonances for coupled PIB chains (Structure V, protons g) are normally found at 4.82 ppm. The methylene protons in the PIBCl end group (Structure VI, protons h) at 1.96 ppm were used to calculate the content of PIBCl. The methylene and methyl protons of the IB repeat unit (Structure I, protons b and c, respectively) were observed at 1.42 and 1.11 ppm,

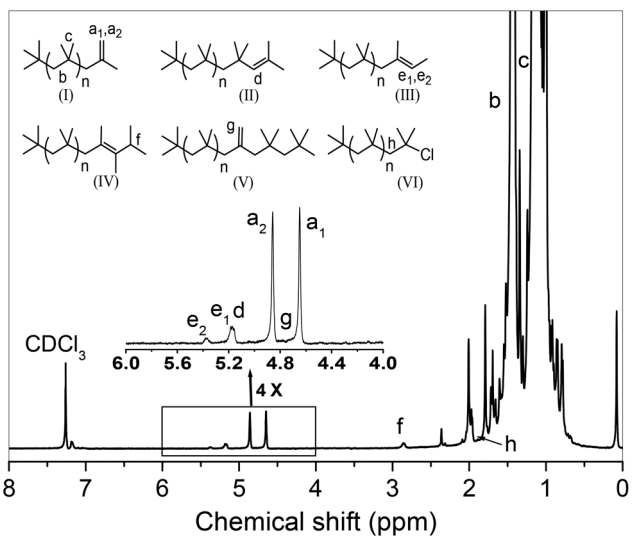

Fig. 1 Typical ^{1}H NMR spectrum of HR PIB obtained in this study using $FeCl_3$·dialkyl ether complexes.

respectively. The number average molecular weights were determined by NMR ($M_{n,NMR}$) using the formula:

$$M_{n,NMR} = 56.11 \times [(b/2)/((a_1 + a_2)/2 + d + e_1 + e_2 + f + (g/2) + (h/2))$$

where 56.11 is the molecular weight of IB, and a_1, a_2, b, *etc.* represents the area corresponding to those protons (Fig. 1).

Density functional calculations

Density functional theory (DFT) calculations were conducted employing the Gaussian 09 package[22] at the B3LYP[23,24] level of theory with Pople's basis set 6-31G*[25–27] for all atoms in the gas phase. The solvent effects of hexane were examined by optimization of the geometries using the polarizable continuum model with the integral equation formalism variant (IEFPCM)[28] with the UAKS model. Different rotamers and spin multiplicities were all calculated and compared, and frequency calculations were performed to locate and confirm those structures as global minima for the binding energy calculation.

Results and discussion

Recently, we reported the polymerization of IB to yield HR PIB initiated by *t*-BuCl and coinitiated by $FeCl_3$·ether complexes in hexane at 0 °C.[19] We have now carried out a more detailed kinetic and mechanistic study. A series of experiments were performed with different complex concentrations and the representative data are shown in Tables 1–3. Additional polymerization data can be found in the ESI Tables S1–S3.† The highest *exo*-olefin content of up to ~80% was achieved with the $FeCl_3$·i-Pr_2O complex. Furthermore the *exo*-olefin content remained relatively constant with time up to 60 min. The $FeCl_3$·CEEE complex gave slightly lower, ~65–75%, *exo*-olefin content that decreased after 20 min, especially at the highest complex concentration due to an increase in the coupled product. The $FeCl_3$·CEE complex resulted in the lowest *exo*-olefin content of ~60%. These results may be attributed to the decreasing basicity of the ethers with i-Pr_2O > CEEE > CEE.

The conversion *versus* time and the first order plots are shown in Fig. 2–4. The substantially higher rates of polymerization for both CEEE and CEE *versus* that of i-Pr_2O, is attributed to the reduced nucleophilicity of these ethers, which increases in the order CEE < CEEE < i-Pr_2O. We previously postulated that the less nucleophilic ether is more easily displaced from the complex, allowing for faster ionization of *t*-BuCl. We have now confirmed this by determining the binding energies of ethers to $FeCl_3$ by DFT calculations (Table 4).

We have previously reported that the polymerization of IB was absent with the $FeCl_3$·Et_2O complex.[18] This is consistent with the high binding energy of this unhindered complex. According to Fig. 2–4 the rate of polymerization increases in the i-Pr_2O < CEEE < CEE order. These findings are in complete agreement with the trend in the calculated binding energies of these ethers to $FeCl_3$. The lower binding energy of i-Pr_2O relative to Et_2O can be explained by steric effects, while the lower binding energies of chloro substituted ethyl ethers are due to electronic effects.

Experimentation was also carried out at different [*t*-BuCl] while [$FeCl_3$·i-Pr_2O] was kept constant at 0.01 M. The results are shown in Table 5 and Fig. 5. At all initiator concentrations a fast polymerization was observed at the initial stage of polymerization and the initial slope of the first order plots were approximately proportional to [*t*-BuCl]. However, all first order plots show a downward curvature.

Although the initial polymerization rates increased with increasing $FeCl_3$·ether and *t*-BuCl concentration as expected, all first order plots are curved suggesting that the PIB^+ concentration decreases during polymerization. The previously

Table 1 Polymerization of [IB] = 1.0 M by $FeCl_3$·i-Pr_2O and [*t*-BuCl] = 0.02 M in hexane at 0 °C. Polymerization time 60 min

#	[$FeCl_3$·iPr_2O] (M)	Conv.[a] (%)	$M_{n,NMR}$[b] (g mol^{-1})	$M_{n,GPC}$[c] (g mol^{-1})	PDI[c]	*exo*[d] (%)	tri + *endo*[d] (%)	tetra[d] (%)	PIB-Cl[d] (%)	Coupled-PIB[d] (%)
1	0.02	100	800	900	2.1	80	9	9	0	2
2	0.01	92	700	1100	2.3	77	9	11	0	3
3	0.005	44	1000	1200	3.0	70	9	12	5	4

[a] Determined gravimetrically based on monomer feed. [b] Determined by NMR analysis. [c] Obtained from SEC measurements. [d] Calculated from NMR spectroscopic study.

Table 2 Polymerization of [IB] = 1.0 M by [$FeCl_3$·CEEE] and [*t*-BuCl] = 0.02 M in hexane at 0 °C. Polymerization time 60 min

#	[$FeCl_3$·CEEE] (M)	Conv.[a] (%)	$M_{n,NMR}$[b] (g mol^{-1})	$M_{n,GPC}$[c] (g mol^{-1})	PDI[c]	*exo*[d] (%)	tri + *endo*[d] (%)	tetra[d] (%)	PIB-Cl[d] (%)	Coupled-PIB[d] (%)
1	0.02	90	300	500	2.3	60	16	9	0	15
2	0.01	100	300	400	2.9	63	14	13	0	10
3	0.005	99	500	600	2.6	64	13	15	0	7

[a] Determined gravimetrically based on monomer feed. [b] Determined from NMR analysis. [c] Obtained from SEC measurements. [d] Calculated from NMR spectroscopic study.

Table 3 Polymerization of [IB] = 1.0 M by [$FeCl_3$·CEE] and [*t*-BuCl] = 0.02 M in hexane at 0 °C. Polymerization time 60 min

#	[$FeCl_3$·CEE] (M)	Conv.[a] (%)	$M_{n,NMR}$[b] (g mol^{-1})	$M_{n,GPC}$[c] (g mol^{-1})	PDI[c]	*exo*[d] (%)	tri + *endo*[d] (%)	tetra[d] (%)	PIB-Cl[d] (%)	Coupled-PIB[d] (%)
1	0.02	95	500	500	2.4	62	20	16	0	2
2	0.01	100	600	700	2.3	55	23	22	0	1
3	0.005	100	900	1000	2.4	50	22	26	0	1

[a] Determined gravimetrically based on monomer feed. [b] Determined from NMR analysis. [c] Obtained from SEC measurements. [d] Calculated from NMR spectroscopic study.

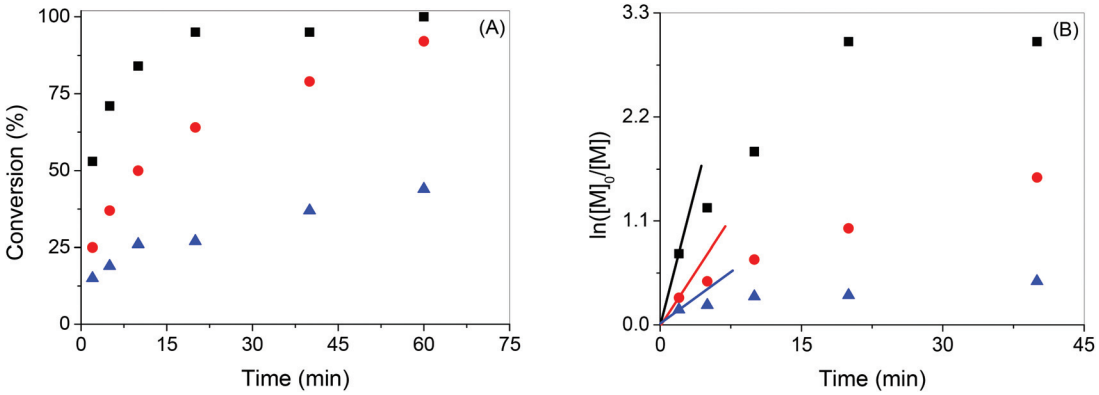

Fig. 2 Polymerization of IB (1.0 M) in the presence of $FeCl_3$·i-Pr_2O and *t*-BuCl (0.02 M) in hexane at 0 °C: (A) conversion *vs.* time plots at different $FeCl_3$·i-Pr_2O concentrations (■: 0.02 M, ●: 0.01 M and ▲: 0.005 M), and (B) corresponding first-order kinetics plots.

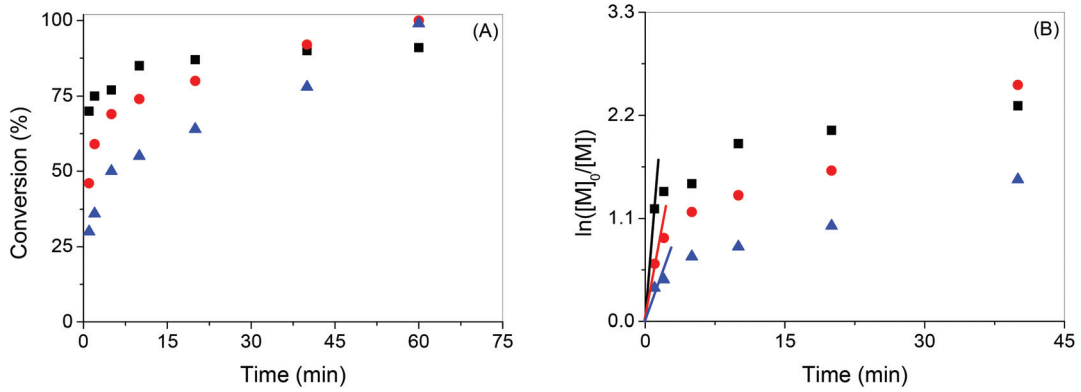

Fig. 3 Polymerization of IB (1.0 M) in the presence of $FeCl_3$·CEEE and *t*-BuCl (0.02 M) in hexane at 0 °C: (A) conversion *vs.* time with different $FeCl_3$·CEEE concentrations (■: 0.02 M, ●: 0.01 M and ▲: 0.005 M), and (B) corresponding first-order kinetics plots.

proposed mechanism is shown in Scheme 1. The first step is initiation: the ionization of *t*-BuCl in the presence of $FeCl_3$·ether and cationation of IB. The propagating macro-cationic species PIB^+ undergoes β-proton elimination to produce PIB *exo*-olefin and the protonated ether $FeCl_4^-$ complex is formed. This protonated ether further transfers the proton to the monomer and polymerization continues.

According to Scheme 1 the polymerization is first order in monomer and the initial polymerization rate is proportional to [*t*-BuCl] and [$FeCl_3$·ROR′]. After all the *t*-BuCl has reacted, the polymerization rate will depend on the rate of chain transfer to IB since the propagation rate constant of IB[29] is close to the diffusion limit and [PIB^+] << [*t*-BuCl]. Thus, in this second stage of the polymerization the concentration of protonated ether should be close to the original [*t*-BuCl] when the starting concentration of the Lewis acid complex and initiator are the same. In order to clarify the mechanism of initiation, polymerization of IB-d_6 was carried out in the presence of [$FeCl_3$·i-Pr_2O] = 0.01 M and [*t*-BuCl] = 0.01 M at 0 °C in hexane. After 30 min, 53% conversion was obtained. ^{1}H NMR spectroscopy was used to confirm initiation from *t*-BuCl (Fig. 6), where we observed *t*-butyl, main chain –CH_2– and chain end –CH_2– protons at 0.99 (9H), 1.39 (*n* × 2H; *n* = number average degrees of polymerization) and 1.99 (2H) ppm, respectively. From the

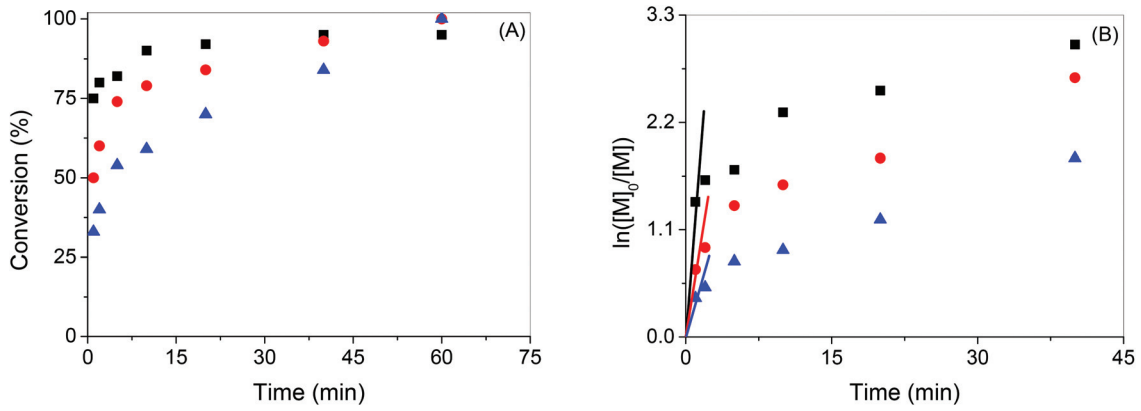

Fig. 4 Polymerization of IB (1.0 M) in the presence of $FeCl_3$·CEE and *t*-BuCl (0.02 M) in hexane at 0 °C: (A) conversion *vs.* time with different $FeCl_3$·CEE concentrations (■: 0.02 M, ●: 0.01 M and ▲: 0.005 M), and (B) corresponding first-order kinetics plots.

Table 4 Calculated binding energies of ethers with $FeCl_3$ (kcal mol^{-1})

Ether	Binding energy in gas phase	Binding energy in hexane
Et_2O	−16.6	−14.3
i-Pr_2O	−15.8	−12.6
CEEE	−13.4	−10.3
CEE	−12.4	−8.1

ratio of peak areas at 1.39 and 0.99 ppm, an $M_{n,NMR}$ = 740 g mol^{-1} was obtained, which is in excellent agreement with the $M_{n,GPC}$ = 730 g mol^{-1} (PDI = 2.6), indicating near-quantitative initiator efficiency with *t*-BuCl.

However, when the complex concentration is lower than the concentration of the initiator (*i.e.* [$FeCl_3$·ROR′] = 0.01 M and [*t*-BuCl] = 0.02 M), half of the initiator would remain unreacted after all of the complex is protonated. Therefore, in the next stage, an experiment with cumyl chloride as an initiator was performed to measure the efficiency of initiation. Cumyl chloride was chosen because the cumyl moiety gives a distinct peak in the ^{1}H NMR spectrum in the range of 7.0–8.0 ppm. We observed 53 and 94% monomer conversions at 0.01 and 0.04 M cumyl chloride concentrations, respectively. According to the ^{1}H NMR spectra (Fig. 7) initiation from cumyl chloride is complete in both cases, because one cumyl group (7.1–7.5 ppm, 5H) is obtained per PIB chain. Also, $M_{n,GPC}$ =

Table 5 Polymerization of [IB] = 1.0 M by [$FeCl_3$·i-Pr_2O] = 0.01 M in hexane at 0 °C at different [*t*-BuCl]. Polymerization time 60 min

#	[*t*-BuCl] (M)	Conv.[a] (%)	$M_{n,NMR}$[b] (g mol^{-1})	$M_{n,GPC}$[c] (g mol^{-1})	PDI[c]	*exo*[d] (%)	tri + *endo*[d] (%)	tetra[d] (%)	PIB-Cl[d] (%)	Coupled-PIB[d] (%)
1	0.01	45	1400	1300	2.3	70	13	16	0	1
2	0.02	60	1300	1200	2.7	68	14	15	0	3
3	0.04	80	1100	1000	2.9	73	11	15	0	1

[a] Determined gravimetrically based on monomer feed. [b] Determined from NMR analysis. [c] Obtained from SEC measurements. [d] Calculated from NMR spectroscopic study.

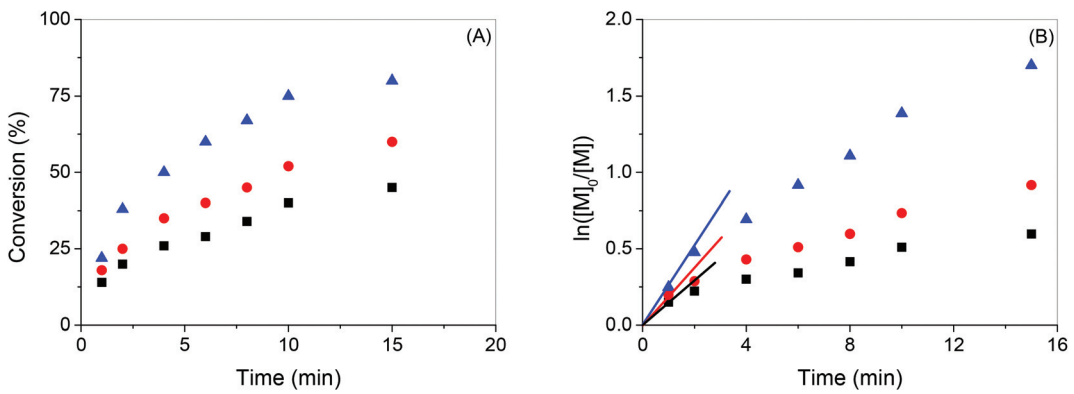

Fig. 5 Polymerization of IB (1.0 M) in the presence of $FeCl_3$·i-Pr_2O (0.01 M) and *t*-BuCl in hexane at 0 °C: (A) conversion *vs.* time plots at different *t*-BuCl concentrations (■: 0.01 M, ●: 0.02 M and ▲: 0.04 M), and (B) corresponding first-order kinetics plots.

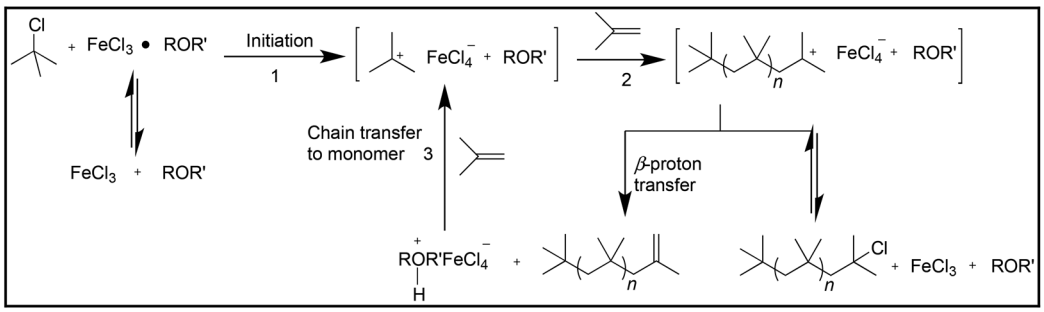

Scheme 1 Proposed mechanism of IB polymerization in the presence of $FeCl_3$·dialkyl ether complexes.

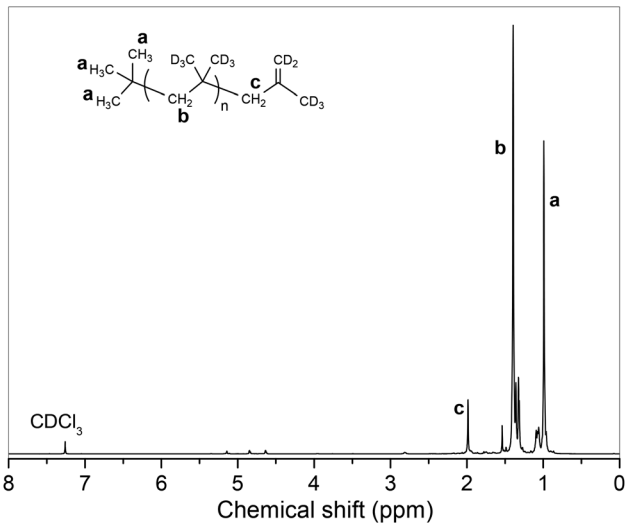

Fig. 6 ^{1}H NMR spectra of polymer obtained from the polymerization of IB-d_6 (1.0 M) in the presence of [$FeCl_3$·i-Pr_2O] = 0.01 M and [*t*-BuCl] = 0.01 M at 0 °C in hexane.

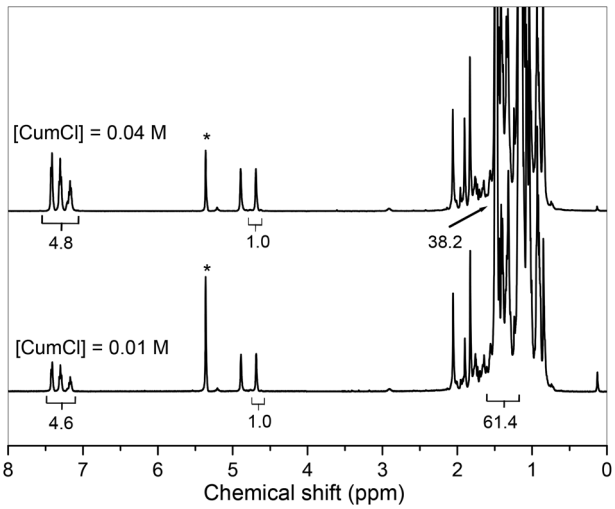

Fig. 7 ^{1}H NMR spectra of PIB obtained from the polymerization of IB (1.0 M) in the presence of [$FeCl_3$·i-Pr_2O] = 0.005 M and cumyl chloride concentrations (0.01 and 0.04 M). *: denote the CD_2Cl_2 resonance.

1300 (PDI = 2.7) and 800 (PDI = 2.4) g mol^{-1} match nicely with the $M_{n,NMR}$ = 1300 and 900 g mol^{-1}, respectively, at 0.01 and 0.04 M cumyl chloride concentrations. These results suggest the existence of the following equilibrium, whereby ionization of the cumyl chloride can proceed and the Lewis base can be regenerated:

$$\text{i-Pr}_2\text{OH}^+\text{FeCl}_4^- \leftrightharpoons \text{HCl} + \text{FeCl}_3 \cdot \text{i-Pr}_2\text{O}$$

This was directly confirmed by ATR FTIR spectroscopy.

Fig. 8 shows the ATR FTIR spectra of $FeCl_3$·i-Pr_2O complex in DCM, and the spectrum observed after purging with dry HCl. (The solubility of the complex in hexane is too low for ATR FTIR spectroscopy.) Upon purging with HCl two new peaks at 912 and 1060 cm^{-1} appeared that are attributed to the protonated $FeCl_3$·i-Pr_2O complex; however, the characteristic C–O–C stretch of the complexed ether at 1100 cm^{-1} did not disappear completely. It is anticipated that in hexane the ratio of protonated/unprotonated complex would be lower. It is also anticipated that the protonated ether salt would have a lower solubility in hexane compared to that of the $FeCl_3$·i-Pr_2O complex.

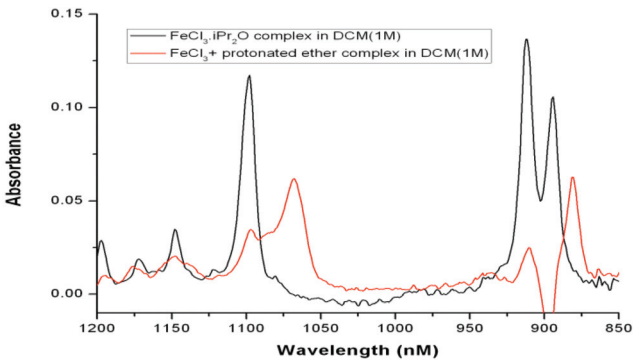

Fig. 8 ATR FTIR spectrum of $FeCl_3$·iPr_2O (in black) and after purging with HCl (in red) in DCM.

Thus a 0.02 M $FeCl_3$·i-Pr_2O complex solution in hexane was purged with HCl. During this process a precipitate was observed. The reaction mixture was transferred to a centrifuge tube and allowed to equilibrate at 0 °C. Then it was spun at 3750 rotations per minute for 10 min; an aliquot of the clear solution was transferred to a round bottom flask, the solvent and any excess ether was removed, and the residue was

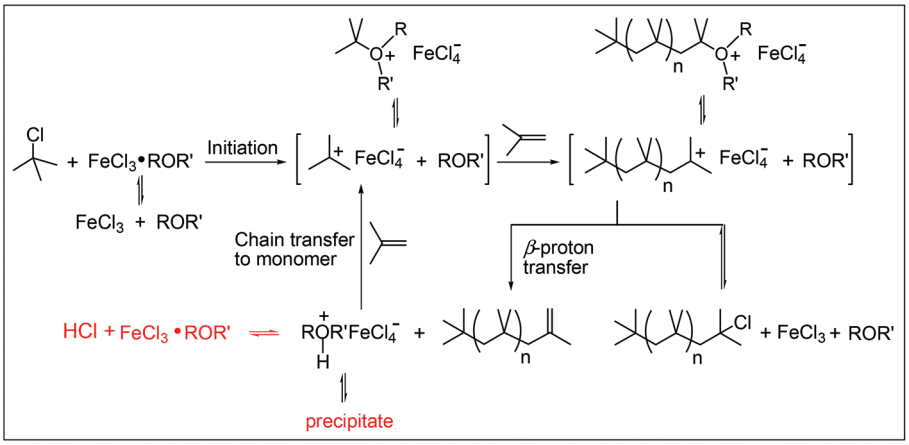

Scheme 2 Revised mechanism of IB polymerization in the presence of $FeCl_3$·dialkyl ether complexes.

weighed. Based on the mass the concentration of hexane soluble protonated and unprotonated complex is 0.0037 M. This is substantially lower than the soluble complex concentration.

According to these findings the proposed mechanism shown in Scheme 1 requires a revision. We now propose a revised mechanism shown in Scheme 2, in which the Lewis acid/ether complex is regenerated from protonated ether by loss of HCl, thereby providing a pathway for ionization of excess initiator. This revised scheme also contains an oxonium ion (dormant species)–carbenium ion (active species) equilibrium postulated in our earlier paper. Ummadisetty and Storey[30] directly observed the oxonium ion formed from the reaction of 2-chloro-2,4,4-trimethylpentane and diisopropyl ether in the presence of excess $TiCl_4$ at −70 °C by ^1H NMR spectroscopy. At low temperature oxonium ion formation is complete and polymerization is absent. The carbenium ion–oxonium ion equilibrium constant is, however, strongly affected by temperature and the stability of the oxonium ion.[31] Although the equilibrium constant for the oxonium ion–carbenium ion equilibrium in Scheme 2 has not yet been determined, the polymerization of IB suggests that oxonium ion (transient species) formation is less than complete.

Conclusion

The rate of the polymerization of IB initiated by *t*-BuCl and coinitiated by $FeCl_3$·ether complexes to yield HR PIB can be increased by decreasing the $FeCl_3$·ether binding energies in the i-Pr_2O > CEEE > CEE order. The cation concentration, however, decreases with time for all three complexes due to precipitation of the protonated complex salt $H^+ROR'FeCl_4^-$, which has a much lower solubility than that of the $FeCl_3$·ether complex. The revised mechanism takes this into account in addition to $H^+ROR'FeCl_4^- \leftrightharpoons$ HCl + $FeCl_3$·ROR′ equilibrium. Thus for the efficient synthesis of HR PIB by Lewis acid·ether complexes, both the complex and the protonated complex salts need to be reasonably soluble. The recently discovered alkylaluminum dichloride·CEE system fulfills these requirements and therefore it is more promising for industrial adoption.[32]

Acknowledgements

Financial support from Infineum USA is greatly acknowledged.

Notes and references

1 F. Balzano, A. Pucci, R. Rausa and G. Uccello-Barretta, *Polym. Int.*, 2012, **61**, 1256–1262.
2 T. V. Liston, *Lubr. Eng.*, 1992, **48**, 389–397.
3 I. Puskas, E. M. Banas and A. G. Nerheim, *J. Polym. Sci., Polym. Symp.*, 1976, **56**, 191–202.
4 I. Puskas and S. Meyerson, *J. Org. Chem.*, 1984, **49**, 258–262.
5 J. J. Harrison, C. M. Mijares, M. T. Cheng and J. Hudson, *Macromolecules*, 2002, **35**, 2494–2500.
6 H. Mach and P. Rath, *Lubr. Sci.*, 1999, **11–2**, 175–185.
7 D. L. Morgan, J. J. Harrison, C. D. Stokes and R. F. Storey, *Macromolecules*, 2011, **44**, 2438–2443.
8 S. Ummadisetty, D. L. Morgan, C. D. Stokes and R. F. Storey, *Macromolecules*, 2011, **44**, 7901–7910.
9 Y. Li, M. Cokoja and F. E. Kuhn, *Coord. Chem. Rev.*, 2011, **255**, 1541–1557.
10 I. V. Vasilenko, D. I. Shiman and S. V. Kostjuk, *Polym. Chem.*, 2014, **5**, 3855–3866.
11 S. V. Kostjuk, H. Y. Yeong and B. Voit, *J. Polym. Sci., Part A: Polym. Chem.*, 2013, **51**, 471–486.
12 M. R. Lichtenthaler, A. Higelin, A. Kraft, S. Hughes, A. Steffani, D. A. Plattner, J. M. Slattery and I. Krossing, *Organometallics*, 2013, **32**, 6725–6735.
13 I. V. Vasilenko, A. N. Frolov and S. V. Kostjuk, *Macromolecules*, 2010, **43**, 5503–5507.
14 Q. Liu, Y.-X. Wu, Y. Zhang, P.-F. Yan and R.-W. Xu, *Polymer*, 2010, **51**, 5960–5969.

15 Q. Liu, Y. Wu, P. Yan, Y. Zhang and R. Xu, *Macromolecules*, 2011, **44**, 1866–1875.
16 A.-R. Guo, X.-J. Yang, P.-F. Yan and Y.-H. Wu, *J. Polym. Sci., Part A: Polym. Chem.*, 2013, **51**, 4200–4212.
17 P. Dimitrov, J. Emert and R. Faust, *Macromolecules*, 2012, **45**, 3318–3325.
18 R. Kumar, P. Dimitrov, K. J. Bartelson, J. Emert and R. Faust, *Macromolecules*, 2012, **45**, 8598–8603.
19 K. J. Bartelson, P. De, R. Kumar, J. Emert and R. Faust, *Polymer*, 2013, **54**, 4858–4863.
20 L. Balogh and R. Faust, *Polym. Bull.*, 1992, **28**, 367–374.
21 After quenching the polymerization, ~0.2 mL ammonium hydroxide solution was added to the polymerization tube at room temperature. Decomposed complex precipitated in the bottom of the tube and the solution was decanted to a 20 mL glass vial. Solvents were removed under the hood, and then the vial was dried at 40 °C under high vacuum for 6 h. Conversions were determined from the initial and final weights of the vial and the IB used during the polymerization.
22 M. J. Frisch, G. W. Trucks, H. B. Schlegel, G. E. Scuseria, M. A. Robb, J. R. Cheeseman, G. Scalmani, V. Barone, B. Mennucci, G. A. Petersson, H. Nakatsuji, M. Caricato, X. Li, H. P. Hratchian, A. F. Izmaylov, J. Bloino, G. Zheng, J. L. Sonnenberg, M. Hada, M. Ehara, K. Toyota, R. Fukuda, J. Hasegawa, M. Ishida, T. Nakajima, Y. Honda, O. Kitao, H. Nakai, T. Vreven, J. J. A. Montgomery, J. E. Peralta, F. Ogliaro, M. Bearpark, J. J. Heyd, E. Brothers, K. N. Kudin, V. N. Staroverov, R. Kobayashi, J. Normand, K. Raghavachari, A. Rendell, J. C. Burant, S. S. Iyengar, J. Tomasi, M. Cossi, N. Rega, N. J. Millam, M. Klene, J. E. Knox, J. B. Cross, V. Bakken, C. Adamo, J. Jaramillo, R. Gomperts, R. E. Stratmann, O. Yazyev, A. J. Austin, R. Cammi, C. Pomelli, J. W. Ochterski, R. L. Martin, K. Morokuma, V. G. Zakrzewski, G. A. Voth, P. Salvador, J. J. Dannenberg, S. Dapprich, A. D. Daniels, Ö. Farkas, J. B. Foresman, J. V. Ortiz, J. Cioslowski and D. J. Fox, *Gaussian 09; Revision A.2*, Gaussian, Inc., Wallingford CT, 2009.
23 A. D. Becke, *J. Chem. Phys.*, 1993, **98**, 5648–5652.
24 C. Lee, W. Yang and R. G. Parr, *Phys. Rev. B: Condens. Matter*, 1988, **37**, 785–789.
25 R. Ditchfield, W. J. Hehre and J. A. Pople, *J. Chem. Phys.*, 1971, **54**, 724–728.
26 W. J. Hehre, R. Ditchfield and J. A. Pople, *J. Chem. Phys.*, 1972, **56**, 2257–2261.
27 P. C. Hariharan and J. A. Pople, *Theor. Chim. Acta*, 1973, **28**, 213–222.
28 S. Miertuš and J. Tomasi, *Chem. Phys.*, 1982, **65**, 239–241.
29 L. Sipos, P. De and R. Faust, *Macromolecules*, 2003, **36**, 8282–8290.
30 S. Ummadisetty and R. F. Storey, *Macromolecules*, 2013, **46**, 2049–2059.
31 St. Penczek and R. Szymański, *Polym. J.*, 1980, **12**, 617–628.
32 R. Kumar, B. Zheng, K.-W. Huang, J. Emert and R. Faust, *Macromolecules*, 2014, **47**, 1959–1965.

